PHYSICAL REVIEW D **92,** 055016 (2015)

Unitarity sum rules, three-site moose model, and the ATLAS 2 TeV diboson anomalies

Tomohiro Abe,[1,*] Ryo Nagai,[2,†] Shohei Okawa,[2,‡] and Masaharu Tanabashi[2,3,§]

[1]*Institute of Particle and Nuclear Studies, High Energy Accelerator Research Organization (KEK), Tsukuba 305-0801, Japan*

[2]*Department of Physics, Nagoya University, Nagoya 464-8602, Japan*

[3]*Kobayashi-Maskawa Institute for the Origin of Particles and the Universe, Nagoya University, Nagoya 464-8602, Japan*

(Received 13 July 2015; published 15 September 2015)

We investigate W' interpretations for the ATLAS 2 TeV diboson anomalies. The roles of the unitarity sum rules, which ensure the perturbativity of the longitudinal vector boson scattering amplitudes, are emphasized. We find the unitarity sum rules and the custodial symmetry are powerful enough to predict various nontrivial relations among WWZ', WZW', WWh, $WW'h$ and $ZZ'h$ coupling strengths in a model independent manner. We also perform surveys in the general parameter space of W' models and find the ATLAS 2 TeV diboson anomalies may be interpreted as a W' particle of the three-site moose model, i.e., a Kaluza-Klein like particle in a deconstructed extra dimension model. It is also shown that the nonstandard-model-like Higgs boson is favored by the present data to interpret the ATLAS diboson anomalies as the consequences of the W' and Z' bosons.

DOI: 10.1103/PhysRevD.92.055016 PACS numbers: 12.60.Cn, 14.70.Pw, 14.80.Rt

I. INTRODUCTION

Recently, the ATLAS Collaboration of the LHC experiment reported anomalies in their search for high-mass diboson (WZ, WW or ZZ) resonances with boson-tagged jets at the diboson invariant mass 2 TeV [1]. W and Z bosons resulting from high-mass resonance are highly boosted, so each boson's hadronic decay products are reconstructed as a single fat jet J in this search. The reported local significances of anomalies are 3.4σ, 2.6σ, and 2.9σ for $WZ \to JJ$, $WW \to JJ$, and $ZZ \to JJ$ channels, respectively. If we explain the ATLAS $WZ \to JJ$ anomaly in the W' model, we need to introduce a narrow high-mass W' boson with $M_{W'} = 2$ TeV, $\Gamma_{W'} < 100$ GeV, and

$$\sigma(pp \to W'; \sqrt{s} = 8 \text{ TeV}) B_{W'}(WZ) \simeq 14 \text{ fb}. \quad (1.1)$$

Note here the above cross section is the best fit value. A W' particle with a little bit smaller production cross section may also be consistent with the ATLAS diboson anomaly.

The CMS Collaboration also reported their results of search for high-mass diboson resonance in the same decay channel [2]. Although the CMS Collaboration reported a small excess around 1.8 TeV, at the resonance mass of 2 TeV, CMS only gives the upper limit on σB, $\sigma(pp \to W'; \sqrt{s} = 8\,\text{TeV}) B_{W'}(WZ) < 13\,\text{fb}$. The ATLAS Collaboration also reported their search for high-mass diboson resonance X in the $WV \to \ell\nu q\bar{q}$ decay channel [3]. Here V stands for W or Z. The ATLAS limit on σB in this decay channel is about

$$\sum_X \sigma(pp \to X; \sqrt{s} = 8 \text{ TeV}) B_X(WV) < 10 \text{ fb}, \quad (1.2)$$

for 2 TeV narrow resonance X. The limit (1.2) causes a tension with the best fit value of the ATLAS diboson anomaly $\sigma(pp \to W') B_{W'}(WZ) \simeq 14$ fb. We use the value $\sigma B \simeq 10$ fb as a reference for our interpretation of the ATLAS diboson anomaly in this paper, though only 70% of the ATLAS diboson excess can be explained with this cross section.

The CMS Collaboration recently reported their search limit on the W' production in the $W' \to Wh \to JJ$ decay channel in Ref. [4]. Although the CMS Collaboration found a small excess of event numbers around $M_{W'} = 1.8$ TeV, they found rather severe upper limit for $M_{W'} = 2$ TeV resonance, i.e., about $\sigma(pp \to W'; \sqrt{s} = 8 \text{ TeV}) B_{W'}(Wh) < 7$ fb. As we will see later, this upper limit causes a severer tension with the ATLAS diboson anomaly. In Ref. [5], the CMS Collaboration reported their search result for high-mass resonance W' in the decay channel $W' \to Wh \to \ell\nu b\bar{b}$. Again, they found an excess at $M_{W'} \simeq 1.8$ TeV.

After the ATLAS Collaboration reported the 2 TeV diboson anomalies [1], many studies of possible theoretical interpretations have appeared in the market [6–17]. One of the biggest questions raised in these interpretations is whether the ATLAS diboson anomaly at $M = 2$ TeV is related with the CMS excesses at $M = 1.8$ TeV or not. Given the situation where the jet mass resolutions of

*abetomo@post.kek.jp
†nagai@eken.phys.nagoya-u.ac.jp
‡okawa@eken.phys.nagoya-u.ac.jp
§tanabash@eken.phys.nagoya-u.ac.jp

ATLAS and CMS detectors are much better than 100 GeV, it seems unlikely that the CMS 1.8 TeV excesses are directly related with the ATLAS 2 TeV anomalies, however. If this is not so, the next theoretical challenge is to make viable models of W' explaining the ATLAS diboson anomalies without causing conflicts with the CMS upper limit on the $W' \to Wh$ decay channel, $\sigma(pp \to W')B_{W'}(Wh) < 7$ fb at $M_{W'} = 2$ TeV. This is a tough challenge, however, if we take the CMS 7 fb upper limit seriously. The Higgs boson is the $SU(2)_W$ partner of the would-be Nambu-Goldstone boson (NGB) in the standard model (SM). The equivalence theorem of the longitudinal W boson and the eaten would-be NGB amplitudes then suggests us a relation

$$\Gamma_{W'}(WZ) = \Gamma_{W'}(Wh) \tag{1.3}$$

for sufficiently heavy W'. See, e.g., Ref. [18] for a typical W' model satisfying this relation (1.3). The relation (1.3) implies that the W' branching fraction to the Wh mode is identical to the W' branching fraction to WZ, i.e., $B_{W'}(WZ) = B_{W'}(Wh)$. The CMS 7 fb upper limit on the Wh channel therefore gives an upper limit on $\sigma(pp \to W')B(WZ) < 7$ fb. Less than only a half of the ATLAS diboson anomaly excess ~14 fb can be explained.

Although this tension may be explained by a statistical fluctuation at the present stage, it is tempting to consider scenarios free from the relation (1.3). In this paper, we point out that the relation (1.3) is true only if the couplings of the 125 GeV Higgs boson with WW and ZZ are same as the SM predictions. We investigate the relation (1.3) from the viewpoint of the perturbative unitarity of the longitudinal W and W' boson scattering amplitudes. We derive a set of unitarity sum rules among coupling strengths of W' and W bosons, which should be satisfied in any perturbative model of W'. We then obtain a relation among the WZW' coupling, the WWh coupling, and the WhW' coupling by using these unitarity sum rules. We find that, if the 125 GeV Higgs is a non-SM Higgs boson, the relation (1.3) should be modified as

$$\kappa_V^2 \Gamma_{W'}(WZ) = \Gamma_{W'}(Wh). \tag{1.4}$$

Here κ_V is defined as $\kappa_V = g_{WWh}/g_{WWh}^{\mathrm{SM}}$, with g_{WWh} and $g_{WWh}^{\mathrm{SM}} = g_W M_W$ being the WWh coupling strength and its corresponding SM value, respectively. The ATLAS 2 TeV diboson anomalies may be consistent with the CMS limits on the Wh decay channel, if we consider a model with $\kappa_V < 1$.[1]

Inspired by the unitarity sum rules and the custodial $SU(2)$ symmetry arguments, we then introduce a parametrization of W' and Z' couplings, and survey the parameter space to find phenomenologically viable models consistent with the existing limits on the W' and Z' particles. We then show that the three-site moose model [19], a linear sigma model generalization of the three-site Higgsless model [20], can explain the parameter space consistent both with the ATLAS anomalies and with the existing limits on W' and Z'. Note that the three-site Higgsless model is a deconstruction [21,22] version of the extra dimension Higgsless model [23]. The gauge symmetry breaking structure of the three-site moose model thus resembles the structure of extra dimension models containing bulk weak gauge fields. The W' and Z' bosons in the three-site moose model can therefore be regarded as the Kaluza-Klein (KK) modes of the weak gauge bosons. We also note that, as emphasized in Ref. [19], the three-site moose model implements a mechanism to adjust the Higgs signal strengths even with $\kappa_V < 1$.

This paper is organized as follows: In Sec. II, we derive a set of unitarity sum rules in a class of models with the custodial symmetry including arbitrary number of custodial $SU(2)$ triplet vector bosons $(W, W', W'', \ldots)$ and neutral Higgs bosons $(h_1, h_2, \ldots)$. We obtain a relationship between the $WW'h$ coupling and the WWh coupling by using the unitarity sum rules. We propose a parametrization for the W' and Z' couplings in a manner consistent with the perturbativity and the custodial symmetry in Sec. III. Surveys in the parameter space of W' and Z' models are presented in Sec. IV. Section V is devoted to the three-site moose model. Summary and outlooks are presented in Sec. VI.

II. UNITARITY SUM RULES

In order to keep the perturbative unitarity in the longitudinal vector boson scattering amplitudes, in any perturbative model, self-interaction coupling strengths of massive vector bosons need to satisfy a set of unitarity sum rules [24–27]. Examples of such unitarity sum rules for a model including a tower of massive vector bosons $(W, W', W'', \ldots)$ are presented in Ref. [28] in the context of the deconstructed Higgsless theory. Unitarity sum rules in a model with W, W' and neutral Higgs bosons $(h_1, h_2, \ldots)$ are discussed in Ref. [19]. See also Refs. [29–32]. In this section, we further generalize the unitarity sum rules of Ref. [19] to obtain a relationship between WWh and $WW'h$ couplings.

A. General sum rules

For simplicity, in this section, we consider the custodial $SU(2)$ symmetry limit. Effects of the custodial symmetry violation arising from the weak hypercharge gauge coupling will be discussed later. The model we consider contains N_V custodial $SU(2)$ triplet vector bosons ($W^a_{i\mu}$, $a = 1, 2, 3$, $i = 0, 1, \ldots, N_V - 1$) and N_h singlet Higgs bosons (h_i, $i = 1, 2, \ldots, N_h$). In order to cancel the E^4-behavior of the longitudinal $W_i W_j \to W_k W_\ell$ scattering

[1]Here we assume existence of mechanism to adjust the Higgs measurement signal strengths with $\kappa_V < 1$.

amplitudes, quartic vector boson coupling strengths $g_{W_iW_jW_kW_\ell}$ need to satisfy

$$g_{W_iW_jW_kW_\ell} = \sum_m g_{W_iW_jW_m} g_{W_kW_\ell W_m}, \tag{2.1}$$

with $g_{W_iW_jW_kW_\ell}$ being symmetric under the exchange of the indices i, j, k, ℓ (Bose symmetry). The triple vector boson couplings also satisfy the Bose symmetry. Here we specified the quartic and triple vector couplings by using notations similar to Ref. [19]. Using (2.1) and the Bose symmetry of $g_{W_iW_jW_kW_\ell}$, it is easy to see

$$\begin{aligned}\sum_m g_{W_iW_jW_m} g_{W_kW_\ell W_m} &= \sum_m g_{W_iW_kW_m} g_{W_jW_\ell W_m} \\ &= \sum_m g_{W_iW_\ell W_m} g_{W_kW_jW_m}.\end{aligned} \tag{2.2}$$

Requiring the cancellation of the E^2-behavior, we also obtain a sum rule which relates the Higgs coupling $g_{W_iW_jh_k}$ with the vector boson self-interaction couplings,

$$\begin{aligned}&\sum_m g_{W_iW_jh_m} g_{W_kW_\ell h_m} \\ &\quad= (M_{W_i}^2 + M_{W_j}^2 + M_{W_k}^2 + M_{W_\ell}^2) g_{W_iW_jW_kW_\ell} \\ &\qquad- \sum_m M_{W_m}^2 g_{W_iW_jW_m} g_{W_kW_\ell W_m} \\ &\qquad- \sum_m M_{W_m}^2 g_{W_iW_kW_m} g_{W_jW_\ell W_m} \\ &\qquad- \sum_m M_{W_m}^2 g_{W_iW_\ell W_m} g_{W_kW_jW_m}.\end{aligned} \tag{2.3}$$

Again we used notations similar to Ref. [19]. We also obtain

$$\begin{aligned}&\sum_m \frac{(M_{W_i}^2 - M_{W_j}^2)(M_{W_k}^2 - M_{W_\ell}^2)}{M_{W_m}^2} g_{W_iW_jW_m} g_{W_kW_\ell W_m} \\ &\quad= \sum_m M_{W_m}^2 (-g_{W_iW_kW_m} g_{W_jW_\ell W_m} \\ &\qquad+ g_{W_iW_\ell W_m} g_{W_kW_jW_m}).\end{aligned} \tag{2.4}$$

Note here that the right-hand side of (2.3) is symmetric under the exchange of the indices i, j, k, ℓ. We therefore obtain

$$\begin{aligned}\sum_m g_{W_iW_jh_m} g_{W_kW_\ell h_m} &= \sum_m g_{W_iW_kh_m} g_{W_jW_\ell h_m} \\ &= \sum_m g_{W_iW_\ell h_m} g_{W_kW_jh_m}.\end{aligned} \tag{2.5}$$

B. Properties of W'

We are now ready to discuss applications of the unitarity sum rules (2.1), (2.2), (2.3), (2.4) and (2.5).

We first consider the sum rule which ensures the cancellation of the E^4-behavior in the $WW \to WW$ amplitude. Equation (2.1) reads

$$g_{WWWW} = g_{WWW}^2 + g_{WWW'}^2. \tag{2.6}$$

We assume here that the sum rule is saturated only by W $(= W_0)$ and W' $(= W_1)$. Effects of possibly existing heavier resonances W'' $(= W_2), \ldots$, are assumed to be negligible.

We should note that the sum rule (2.6) is incomplete below the energy scale $E \lesssim M_{W'}$, where the W' exchange term $g_{WWW'}^2$ does not affect the $WW \to WW$ amplitude. The longitudinal polarization of W gives a factor E/M_W in the amplitude for $E \gg M_W$. For the energy scale $M_{W'} \gtrsim E \gg M_W$, the $WW \to WW$ amplitude therefore behaves as

$$(g_{WWWW} - g_{WWW}^2) \frac{E^4}{M_W^4}. \tag{2.7}$$

Requiring the amplitude is still in a perturbative regime [33] at $E = M_{W'}$, we obtain a condition

$$(g_{WWWW} - g_{WWW}^2) \frac{M_{W'}^4}{M_W^4} \lesssim 32\pi. \tag{2.8}$$

It is now easy to see that the $g_{WWW'}$ coupling needs to satisfy

$$g_{WWW'}^2 \frac{M_{W'}^4}{M_W^4} \lesssim 32\pi. \tag{2.9}$$

Parametrizing the $g_{WWW'}$ coupling

$$g_{WWW'} = \xi_V g_{WWW} \frac{M_W^2}{M_{W'}^2}, \tag{2.10}$$

the perturbativity condition (2.9) can be expressed as

$$|\xi_V| \lesssim 15. \tag{2.11}$$

Here we used $g_{WWW} \simeq 0.65$. In typical analyses of collider phenomenologies of W', the parameter ξ_V is chosen to be $\xi_V \simeq 1$. Although this choice clearly satisfies the perturbativity condition (2.11), it is also possible to construct models with larger value of ξ_V, e.g., $\xi_V \sim 5$, still keeping the perturbativity condition (2.9).

We next consider the sum rule which ensures the cancellation of the E^4-behavior in the $WW \to W'W'$ amplitude, Eq. (2.2),

$$g_{WW'W}^2 + g_{WW'W'}^2 = g_{WWW} g_{W'W'W} + g_{WWW'} g_{W'W'W'}. \tag{2.12}$$

Equation (2.12) can be regarded as a quadratic equation of $g_{WW'W'}$,

$$0 = g^2_{WW'W'} - g_{WWW}g_{WW'W'} + g^2_{WWW'} - g_{W'W'W'}g_{WWW'}. \quad (2.13)$$

Plugging (2.10) into (2.13), we obtain

$$0 = g^2_{WW'W'} - g_{WWW}g_{WW'W'} + \xi_V^2 g^2_{WWW}\frac{M_W^4}{M_{W'}^4} - \xi_V g_{W'W'W'}g_{WWW}\frac{M_W^2}{M_{W'}^2}. \quad (2.14)$$

Solving the quadratic equation (2.14) in the $M_{W'}^2 \gg M_W^2$ limit, we obtain two solutions

$$g_{WW'W'} = g_{WWW}, \quad (2.15)$$

or

$$g_{WW'W'} = -\xi_V g_{W'W'W'}\frac{M_W^2}{M_{W'}^2}. \quad (2.16)$$

We next turn to the properties of Higgs couplings g_{WWh_m} and $g_{WW'h_m}$. Let us start with the E^2 sum rule for the $WW \to WW$ amplitude. Using (2.3) we obtain

$$\sum_m g^2_{WWh_m} = 4M_W^2(g^2_{WWW} + g^2_{WWW'}) - 3M_W^2 g^2_{WWW} - 3M_{W'}^2 g^2_{WWW'}, \quad (2.17)$$

where (2.1) is also used to rewrite the quartic vector boson coupling strength g_{WWWW} in terms of g_{WWW} and $g_{WWW'}$. Plugging (2.10) into (2.17), we find

$$\sum_m g^2_{WWh_m} = M_W^2 g^2_{WWW}\left[1 - 3\xi_V^2\frac{M_W^2}{M_{W'}^2}\right]. \quad (2.18)$$

The Higgs boson coupling with the WW state is therefore affected by the parameter ξ_V and the W' boson mass. The roles of the unitarity sum rule (2.18) have been widely studied in Refs. [29–32].

The E^2 sum rules for the $WW \to WW'$ amplitude can also be derived from (2.3),

$$\sum_m g_{WWh_m}g_{WW'h_m} = (3M_W^2 + M_{W'}^2)[g_{WWW}g_{WW'W} + g_{WWW'}g_{WW'W'}] - 3M_W^2 g_{WWW}g_{WW'W} - 3M_{W'}^2 g_{WWW'}g_{WW'W'} = M_{W'}^2 g_{WWW}g_{WWW'} + (3M_W^2 - 2M_{W'}^2)g_{WWW'}g_{WW'W'}. \quad (2.19)$$

Putting the parametrization of $g_{WWW'}$ (2.10) and one solution of $g_{WW'W'}$ (2.15) into (2.19), we obtain

$$\sum_m g_{WWh_m}g_{WW'h_m} = -\xi_V M_W^2 g^2_{WWW}\left[1 + \mathcal{O}\left(\frac{M_W^2}{M_{W'}^2}\right)\right]. \quad (2.20)$$

If we put (2.10) and the other solution of $g_{WW'W'}$ (2.16), we find

$$\sum_m g_{WWh_m}g_{WW'h_m} = \xi_V M_W^2 g^2_{WWW}\left[1 + \mathcal{O}\left(\frac{M_W^2}{M_{W'}^2}\right)\right]. \quad (2.21)$$

For the $WW \to W'W'$ scattering, not only (2.3) but also (2.4) gives nontrivial sum rules. From (2.3), we obtain

$$\begin{aligned}\sum_m g^2_{WW'h_m} &= (2M_W^2 + 2M_{W'}^2)[g^2_{WW'W} + g^2_{WW'W'}] \\ &\quad - 2[M_W^2 g^2_{WW'W} + M_{W'}^2 g^2_{WW'W}] \\ &\quad - [M_W^2 g_{WWW}g_{W'W'W} + M_{W'}^2 g_{WWW'}g_{W'W'W'}] \\ &= 2M_{W'}^2 g^2_{WWW'} + 2M_W^2 g^2_{WW'W'} \\ &\quad - [M_W^2 g_{WWW}g_{WW'W'} + M_{W'}^2 g_{WWW'}g_{W'W'W'}]. \end{aligned} \quad (2.22)$$

We also obtain from (2.4)

$$\begin{aligned}&\frac{(M_W^2 - M_{W'}^2)^2}{M_W^2}g^2_{WW'W} + \frac{(M_W^2 - M_{W'}^2)^2}{M_{W'}^2}g^2_{WW'W'} \\ &= M_W^2(g^2_{WW'W} - g_{WWW}g_{W'W'W}) \\ &\quad + M_{W'}^2(g^2_{WW'W'} - g_{WWW'}g_{W'W'W'}), \end{aligned} \quad (2.23)$$

which reads

$$\begin{aligned}&M_W^2 g_{WWW}g_{WW'W'} + M_{W'}^2 g_{WWW'}g_{W'W'W'} \\ &= \left[M_W^2 - \frac{(M_W^2 - M_{W'}^2)^2}{M_W^2}\right]g_{WWW'} \\ &\quad + \left[M_{W'}^2 - \frac{(M_W^2 - M_{W'}^2)^2}{M_{W'}^2}\right]g_{WW'W'}. \end{aligned} \quad (2.24)$$

Note that the last line of (2.22) can be erased by using (2.24). We now have

$$\sum_m g^2_{WW'h_m} = \frac{M_{W'}^4}{M_W^2}g^2_{WWW'} + \frac{M_W^4}{M_{W'}^2}g^2_{WW'W'}. \quad (2.25)$$

It is now easy to show

$$\sum_m g^2_{WW'h_m} = \xi_V^2 M_W^2 g^2_{WWW}\left[1 + \mathcal{O}\left(\frac{M_W^2}{M_{W'}^2}\right)\right]. \quad (2.26)$$

Combining (2.18), (2.20) and (2.26), we obtain an impressive sum rule

$$\frac{1}{M_W^2}\sum_m (g_{WW'h_m} + \xi_V g_{WWh_m})^2 = \xi_V^2 g_{WWW}^2 \mathcal{O}\left(\frac{M_W^2}{M_{W'}^2}\right). \tag{2.27}$$

Similarly, using (2.21) instead of (2.20), we find

$$\frac{1}{M_W^2}\sum_m (g_{WW'h_m} - \xi_V g_{WWh_m})^2 = \xi_V^2 g_{WWW}^2 \mathcal{O}\left(\frac{M_W^2}{M_{W'}^2}\right). \tag{2.28}$$

For both cases, we obtain

$$g_{WW'h_m} = \pm\xi_V\left[g_{WWh_m} \pm g_{WWh}^{\rm SM}\mathcal{O}\left(\frac{M_W}{M_{W'}}\right)\right]. \tag{2.29}$$

We used here $g_{WWh}^{\rm SM} \simeq g_{WWW}M_W$. The Higgs ($h$) coupling with WW' is therefore related with $g_{WWW'}$ and g_{WWh} through the relation (2.29) in the large $M_{W'}$ limit. If the coupling of the 125 GeV Higgs boson (h) $g_{WWh} \simeq g_{WWh}^{\rm SM}$, we find the uncertainty in (2.29) is about 4% ($= M_W/M_{W'}$) for $M_{W'} = 2$ TeV and therefore is negligibly small.

We note (2.29) is a novel relation, which has not been pointed out in earlier references. The relation provides us further information for the W' boson properties beyond the widely studied $WW \to WW$ sum rule (2.18). We emphasize that we provided the proof of (2.29) in models with arbitrary number of the neutral Higgs bosons. Another remark is that the conclusion (2.29) is unchanged even if we consider models containing W'' or higher KK resonances. The result (2.29) can therefore be applied to a large class of perturbative models which include the W' particle and neutral Higgs bosons.

III. UNITARITY INSPIRED PARAMETRIZATION FOR W' AND Z'

In the previous section, we have shown that the coupling strengths of the W' boson can be controlled by the perturbative unitarity requirements in the custodial $SU(2)$ symmetric model. Especially, we found

$$g_{WWW'} = \xi_V g_{WWW}\frac{M_W^2}{M_{W'}^2}, \qquad \xi_V \lesssim 15, \tag{3.1}$$

and

$$g_{WW'h_m} = \pm\xi_V g_{WWh_m}. \tag{3.2}$$

In this section, we consider effects of custodial $SU(2)$ symmetry violation $M_Z \neq M_W$, $M_{Z'} \neq M_{W'}$, requiring the high energy E^2-behavior of the longitudinal W and Z boson scattering amplitudes are custodial $SU(2)$ symmetric. This requirement is justified because the weak hypercharge coupling (the origin of the custodial symmetry violation) does not affect the E^2-behavior in the amplitudes at the tree level. We find (3.1) needs to be modified as[2]

$$g_{WZW'} = \xi_V g_W \frac{M_W M_Z}{M_{W'}^2}. \tag{3.3}$$

$$g_{WWZ'} = \xi_V g_W \frac{M_W^2}{M_{Z'}^2}R, \tag{3.4}$$

with $R(M_{W'}/M_{Z'})$ being a function of $M_{W'}/M_{Z'}$ satisfying $R(1) = 1$. Here g_W stands for the gauge coupling strength of the W boson.

The Higgs couplings with the WW' and ZZ' states can also be parametrized by using the custodial $SU(2)$ symmetry. We obtain

$$g_{WW'h} = \xi_h g_W M_W, \tag{3.5}$$

$$g_{ZZ'h} = \xi_h g_W M_Z R, \tag{3.6}$$

with h being the 125 GeV Higgs boson. The requirement of the perturbative unitarity then leads to

$$\xi_h = \pm\kappa_V\xi_V, \qquad \kappa_V \equiv \frac{g_{WWh}}{g_W M_W} \tag{3.7}$$

as we have shown in the previous section. It is now straightforward to show the relation (1.4). The relation (3.7) and therefore (1.4) should be regarded as one of the most important unitarity relations obtained in this paper. We are now able to describe the physics of W, W' and Higgs by using the two parameters (κ_V and ξ_V), instead of the three (κ_V, ξ_V and ξ_h).

In order to study collider phenomenologies of W' and Z' particles, we need to specify the couplings of W' and Z' with quarks and leptons. In this paper we adopt an ansatz in which W' and Z' couple with weak current of quarks (leptons) with universal coupling strength $\xi_q g_W$ ($\xi_\ell g_W$). An example of a model satisfying this ansatz will be introduced in Sec. V.

IV. FIT TO THE ATLAS DIBOSON ANOMALY

We are now ready to search the parameter region of ξ_V, ξ_q, and ξ_ℓ so as to explain the ATLAS 2 TeV diboson anomaly in W' models. As we discussed in Sec. I, we use

$$\sum_X \sigma(pp \to X)B_X(VV) \simeq 10\ \text{fb}, \tag{4.1}$$

as a reference value to explain the ATLAS 2 TeV diboson anomaly. Here X is a narrow width new particle having 2 TeV mass decaying to the VV states, with V being a weak

[2]The default value of the PYTHIA [34] implementation of the extended gauge model [35] corresponds to $\xi_V = M_W^2/M_Z^2$.

gauge boson W or Z. The ATLAS Collaboration reported excesses not only in the WZ category, but also in the WW and ZZ categories. It has being claimed that there exist significant size of event contamination among WZ, WW and ZZ categories in the JJ events [6,14], however. We therefore evaluate

$$\sum_{X=W',Z'} \sigma(pp \to X) B_X(VV) \tag{4.2}$$

for a degenerated W' and Z' model ($M_{W'} = M_{Z'} = 2$ TeV), and

$$\sigma(pp \to W') B_{W'}(WZ) \tag{4.3}$$

for a nondegenerated model ($M_{Z'} > M_{W'} = 2$ TeV), and simply compare the number with the reference value (4.1).

In addition to σB, we also need to explain the narrow width of the new particle X, typically smaller than the bin size of the experiment [1], 100 GeV.

The model explaining the diboson anomaly needs to be consistent with the existing limits on the W' and Z' bosons. Both ATLAS and CMS experiments report upper limits on the production cross section of W' in its leptonic decay channels [36,37]. For 2 TeV W' boson search in pp collisions at $\sqrt{s} = 8$ TeV, the limit is

$$\sigma(pp \to W') B_{W'}(\ell\nu) \lesssim 0.4 \text{ fb}. \tag{4.4}$$

Limits on the $Z' \to e^+e^-, \mu^+\mu^-$ are reported in Refs. [38,39]. For $M_{Z'} = 2$ TeV, these references give a limit

$$\sigma(pp \to Z') B_{Z'}(\ell^+\ell^-) \lesssim 0.2 \text{ fb}. \tag{4.5}$$

The LHC limits on the resonant dijet production can also be used to constrain W' models. Using the limits presented in Refs. [40,41], we see

$$\sum_{X=W',Z'} \sigma(pp \to X) B_X(2j) \lesssim 100 \text{ fb}, \tag{4.6}$$

for a degenerated $M_{W'} = M_{Z'} = 2$ TeV model, and

$$\sigma(pp \to W') B_{W'}(2j) \lesssim 100 \text{ fb}, \tag{4.7}$$

for a nondegenerated model with $M_{W'} = 2$ TeV.

Finally, the model needs to satisfy the limit on the $W' \to Wh$ and $Z' \to Zh$ decay modes. Here h stands for the 125 GeV Higgs particle. The limit quoted in Ref. [4] is

$$\sum_{X=W',Z'} \sigma(pp \to X) B_X(Vh) \lesssim 7 \text{ fb}, \tag{4.8}$$

for $M_{W'} = M_{Z'} = 2$ TeV, and

$$\sigma(pp \to W') B_{W'}(Wh) \lesssim 7 \text{ fb}, \tag{4.9}$$

for a nondegenerated model with $M_{W'} = 2$ TeV.

Figure 1 shows these limits in the $\xi_f - \xi_V$ plane for $M_{Z'} = M_{W'} = 2$ TeV. We assume quark-lepton universal coupling $\xi_f = |\xi_q| = |\xi_\ell|$ in this plot. We also assume the 125 GeV Higgs coupling with WW' and ZZ' are given by

$$\xi_h = \pm \xi_V, \tag{4.10}$$

which corresponds to $\kappa_V = 1$ in the unitarity relation (3.7). The dijet limit (4.6) is applied for the resonant production cross section of five flavor $q\bar{q}$ pairs. The W' and Z' particles are produced through their couplings with quarks in pp collisions at 8 TeV. The production cross sections are evaluated by using the CTEQ6L1 set of the parton distribution functions [42].

We see in this plot that the Higgs mode limit (4.8) and the leptonic decay mode limit (4.4) rule out huge parameter space. It is impossible to obtain the reference value of the cross section (4.1) without causing conflicts with the Higgs mode limit (4.8) under the Higgs coupling assumption (4.10). We are only able to achieve $\sum_{X=W',Z'} \sigma(X) B_X(VV) \simeq$ 7 fb at most.

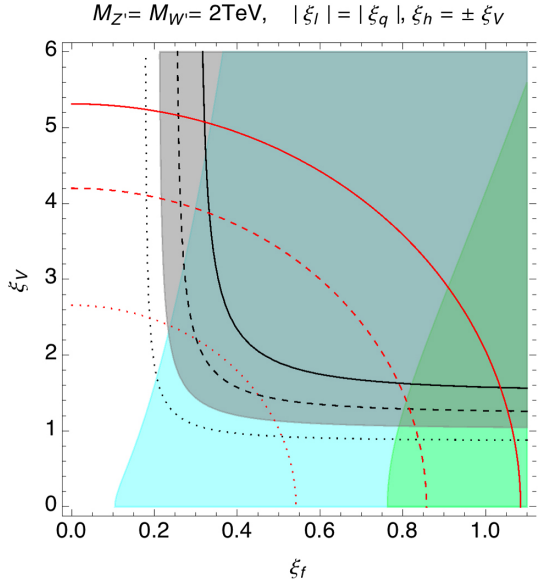

FIG. 1 (color online). Limits on the W' and Z' couplings in the $\xi_f - \xi_V$ plane for the degenerated $M_{Z'} = M_{W'} = 2$ TeV model. $\xi_f = |\xi_q| = |\xi_\ell|$ and $\xi_h = \pm\xi_V$ are assumed. The dark green region, the light blue region, and the gray region are excluded by the dijet mode limit (4.6), the $\ell\nu$ mode (4.4), and Higgs mode (4.8), respectively. Although we do not show the limit from (4.5) in the plot, it is numerically almost identical to the $W' \to \ell\nu$ limit. The black solid curve, the black dashed curve, and the black dotted curve are for $\sigma(pp \to W') B_{W'}(WZ) + \sigma(pp \to Z') B_{Z'}(WW) = 15$ fb, 10 fb, and 5 fb, respectively. The red solid curve, the red dashed curve, and the red dotted curve are for $\Gamma_{W'} = 80$ GeV, 50 GeV, and 20 GeV, respectively. The width of Z' is almost equal to $\Gamma_{W'}$ thanks to the custodial symmetry.

A similar plot for a leptophobic $\xi_\ell = 0$ model is shown in Fig. 2 assuming the degenerated W' and Z', $M_{Z'} = M_{W'} = 2$ TeV. Again, the 125 GeV Higgs coupling is assumed to satisfy (4.10). Although the constraints from the leptonic decay channels of W' and Z' disappear in the leptophobic model, the limit on the Vh channel gives severe constraint on (4.2). It is impossible to obtain the reference value 10 fb in this setup.

In order to explain the diboson excess without causing conflicts with the Higgs mode limit (4.8), we need to take smaller value of ξ_h. The unitarity relation (3.7) suggests such a value of ξ_h can be achieved only if we consider models with a non-SM-like Higgs ($\kappa_V < 1$). Figure 3 shows the plot with $\xi_h/\xi_V = \pm 0.7$, i.e., $\kappa_V = 0.7$. The quark-lepton universal couplings $\xi_f = |\xi_q| = |\xi_\ell|$ are assumed in the plot. The reference cross section value for the excess can be explained at, e.g., $\xi_V \simeq 4$ and $\xi_f \simeq 0.23$. Note that the choice of this parameter ξ_V satisfies the perturbativity condition (2.11).

We next consider the nondegenerated case, $M_{Z'} > M_{W'} = 2$ TeV. The Z' boson is assumed to be heavy enough to be separated from the 2 TeV resonance. The plot corresponding to this model is shown in Fig. 4.

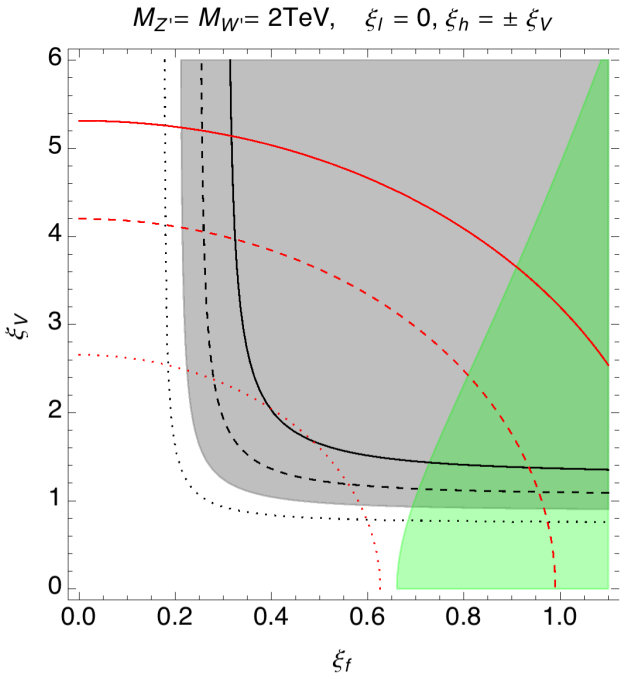

FIG. 2 (color online). Plot similar to Fig. 1 for leptophobic case $\xi_\ell = 0$, $\xi_f = |\xi_q|$. $\xi_h = \pm\xi_V$ is assumed. The dark green region, and the gray region are excluded by the dijet mode limit (4.6), and Higgs mode (4.8), respectively. The black solid curve, the black dashed curve, and the black dotted curve are for $\sigma(pp \to W')B_{W'}(WZ) + \sigma(pp \to Z')B_{Z'}(WW) = 15$ fb, 10 fb, and 5 fb, respectively. The red solid curve, the red dashed curve, and the red dotted curve are for $\Gamma_{W'} = 80$ GeV, 50 GeV, and 20 GeV, respectively. The width of Z' is almost equal to $\Gamma_{W'}$ thanks to the custodial symmetry.

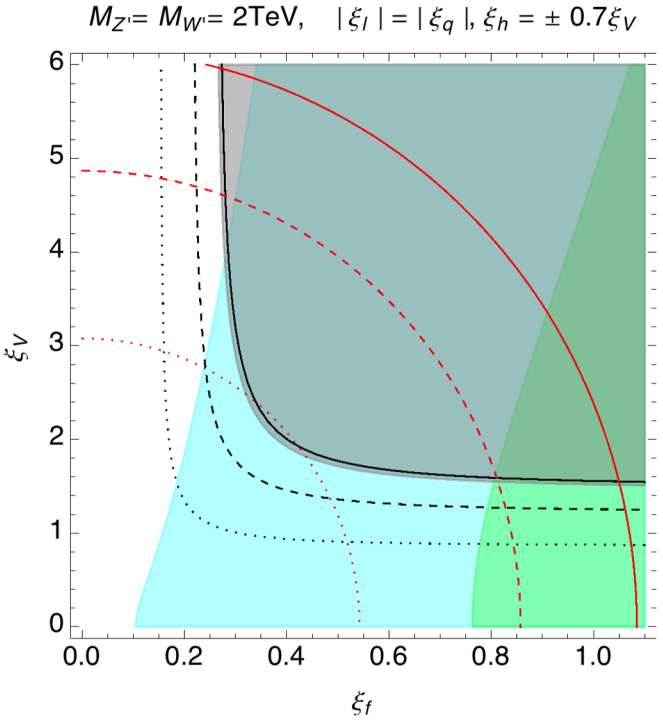

FIG. 3 (color online). Plot similar to Fig. 1 for $\xi_h/\xi_V = \pm 0.7$. $\xi_f = |\xi_q| = |\xi_\ell|$ is assumed. The dark green region, the light blue region, and the gray region are excluded by the dijet mode limit (4.6), the $\ell\nu$ mode (4.4), and Higgs mode (4.8), respectively. Although we do not show the limit from (4.5) in the plot, it is numerically almost identical to the $W' \to \ell\nu$ limit. The black solid curve, the black dashed curve, and the black dotted curve are for $\sigma(pp \to W')B_{W'}(WZ) + \sigma(pp \to Z')B_{Z'}(WW) = 15$ fb, 10 fb, and 5 fb, respectively. The red solid curve, the red dashed curve, and the red dotted curve are for $\Gamma_{W'} = 80$ GeV, 50 GeV, and 20 GeV, respectively. The width of Z' is almost equal to $\Gamma_{W'}$ thanks to the custodial symmetry.

Here $\xi_f = |\xi_\ell| = |\xi_q|$ and $\xi_h/\xi_V = \pm 0.7$ are assumed. We find that the reference cross section value for the ATLAS diboson anomaly can be explained at, e.g., $\xi_V \simeq 4$ and $\xi_f \simeq 0.28$.

A plot similar to Figs. 1, 2, and 3 is also presented in Ref. [6] in the context of the techni-ρ interpretation for the ATLAS diboson anomalies. The plot presented in the latest version of Ref. [6] seems to be consistent with our results.

V. THREE-SITE MOOSE MODEL

So far, we have analyzed the unitarity sum rules and the interpretations of the LHC anomaly of the diboson resonance in terms of W' and Z' without writing an explicit gauge invariant Lagrangian.

In this section, we introduce the three-site moose model [20] as an example to explain the ATLAS diboson excess in a perturbative manner. We are able to check explicitly that the unitarity sum rules are satisfied in the three-site moose model. We also find that the parameter region explaining

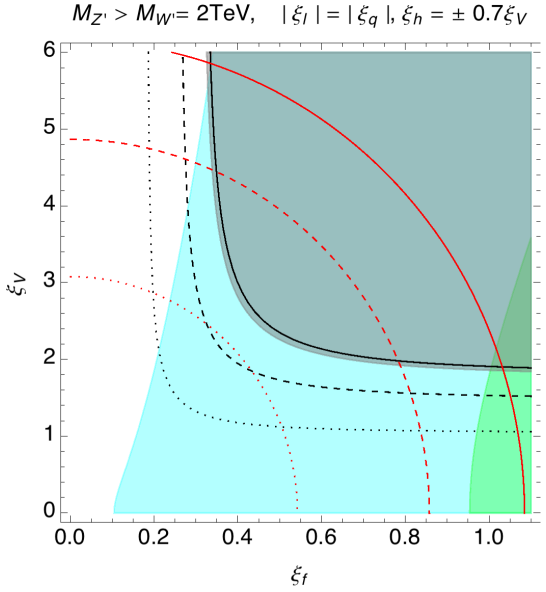

FIG. 4 (color online). Plot similar to Fig. 1 for nondegenerated model $M_{Z'} > M_{W'} = 2$ TeV with $\xi_h/\xi_V = \pm 0.7$. $\xi_f = |\xi_q| = |\xi_\ell|$ is assumed. The dark green region, the light blue region, and the gray region are excluded by the dijet mode limit (4.6), the $\ell\nu$ mode (4.4), and Higgs mode (4.9), respectively. The black solid curve, the black dashed curve, and the black dotted curve are for $\sigma(pp \to W')B_{W'}(WZ) = 15$ fb, 10 fb, and 5 fb, respectively. The red solid curve, the red dashed curve, and the red dotted curve are for $\Gamma_{W'} = 80$ GeV, 50 GeV, and 20 GeV, respectively.

the ATLAS diboson anomaly is naturally realized in this model.

The three-site moose model [20] was originally introduced as a deconstruction version of the Higgsless theory [23]. This model contains W' and Z' bosons as KK particles of electroweak gauge bosons. These KK particles are, at least partly, responsible for the unitarization of the longitudinal weak gauge boson scattering amplitudes [23,43,44]. After the LHC discovery of the 125 GeV Higgs boson, the three-site moose model was extended to include the 125 GeV Higgs particle in Ref. [19]. This model can be regarded as a benchmark model to study the phenomenologies of W' and Z' particles.

The structure of gauge symmetry breaking in the three-site moose model is illustrated in the "moose notation" [45] in Fig. 5. In the three-site moose model, we introduce

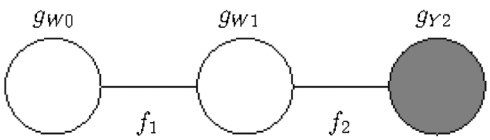

FIG. 5. The moose diagram for the three-site model. The blank circles represent $SU(2)$ gauge groups, with coupling strengths g_{W0} and g_{W1}, and the shaded circle is a $U(1)$ gauge group with coupling g_{Y2}.

$SU(2)_{W0} \times SU(2)_{W1} \times U(1)_{Y2}$ gauge groups. The line connecting the $SU(2)_{W0}$ group with the $SU(2)_{W1}$ group in the moose diagram represents bifundamental (2×2 matrix) Higgs field Φ_1,

$$\Phi_1 = S_1 \mathbf{1} + i\tau^a \pi_1^a, \tag{5.1}$$

with τ^a being the Pauli spin matrix. Similarly, the line between the $SU(2)_{W1}$ and $U(1)_{Y2}$ gauge groups corresponds to the Higgs field Φ_2

$$\Phi_2 = S_2 \mathbf{1} + i\tau^a \pi_2^a. \tag{5.2}$$

The covariant derivatives of Φ_1 and Φ_2 are given by

$$D_\mu \Phi_1 = \partial_\mu \Phi_1 + i g_{W0} W_{0\mu} \Phi_1 - i g_{W1} \Phi_1 W_{1\mu}, \tag{5.3}$$

$$D_\mu \Phi_2 = \partial_\mu \Phi_2 + i g_{W1} W_{1\mu} \Phi_2 - i g_{Y2} \Phi_2 \frac{\tau^3}{2} B_\mu. \tag{5.4}$$

Here $W_{0\mu} = W_{0\mu}^a \frac{\tau^a}{2}$, $W_{1\mu} = W_{1\mu}^a \frac{\tau^a}{2}$, and B_μ are the gauge fields of $SU(2)_{W0}$, $SU(2)_{W1}$, and $U(1)_{Y2}$.

The Higgs field Φ_1 is assumed to acquire its vacuum expectation value (VEV),

$$\langle \Phi_1 \rangle = f_1 \mathbf{1}, \tag{5.5}$$

which breaks the $SU(2)_{W0} \times SU(2)_{W1}$ into the diagonal subgroup $SU(2)$. Similarly, the $SU(2)_{W1} \times U(1)_{Y2}$ is broken to $U(1)$ thanks to the VEV of Φ_2,

$$\langle \Phi_2 \rangle = f_2 \mathbf{1}. \tag{5.6}$$

Simultaneous existence of two VEVs $f_1 \neq 0$ and $f_2 \neq 0$ therefore leads to the spontaneous symmetry breaking pattern

$$SU(2)_{W0} \times SU(2)_{W1} \times U(1)_{Y2} \to U(1)_{\text{em}}. \tag{5.7}$$

Diagonalizing the mass matrices of $W_{0\mu}$, $W_{1\mu}$, and B_μ which arise from the Higgs kinetic term Lagrangian

$$\mathcal{L} \ni \frac{1}{4} \text{tr}[(D_\mu \Phi_1)^\dagger (D^\mu \Phi_1)] + \frac{1}{4} \text{tr}[(D_\mu \Phi_2)^\dagger (D^\mu \Phi_2)], \tag{5.8}$$

we obtain mass eigenstates, W', Z' (heavier massive charged and neutral vector bosons), W, Z (lighter massive vector bosons), and a massless photon.

The weak hypercharge gauge couplings of quarks and leptons are given by

$$\mathcal{L} \ni - J^\mu_{Y,\text{quark}} B_\mu - J^\mu_{Y,\text{lepton}} B_\mu. \tag{5.9}$$

As shown in Ref. [20], after the gauge symmetry breaking, the weak currents of quarks and leptons can be

"delocalized" with delocalization parameters x_q and $x_\ell (0 \le x_q \le 1, 0 \le x_\ell \le 1)$,

$$\mathcal{L} \ni - J^{a\mu}_{W,\text{quark}} (g_{W0} W^a_{0\mu} (1 - x_q) + g_{W1} W^a_{1\mu} x_q) - J^{a\mu}_{W,\text{lepton}} (g_{W0} W^a_{0\mu} (1 - x_\ell) + g_{W1} W^a_{1\mu} x_\ell). \tag{5.10}$$

We should emphasize here that the weak current of quarks and leptons couples with both $SU(2)_{W0}$ and $SU(2)_{W1}$ in Eq. (5.10). This phenomenon called "delocalization" is characteristic in extra dimension scenarios [46], in which KK quarks and KK leptons exist. A similar phenomenon also realizes in the partial compositeness scenarios [47] in which the role of the KK fermions is played by the composite fermions. This is in contrast to the conventional G221 models including the right-handed $SU(2)$ model, in which the weak current cannot be delocalized.

The delocalization parameters x_q and x_ℓ need to be flavor universal in order to avoid the flavor-changing-neutral-current constraints in the three-site model [48]. The quark delocalization parameter x_q can differ from the lepton parameter x_ℓ, however. The electroweak precision constraints can be satisfied for heavy enough W' and Z'. Even with lighter $M_{W'} \lesssim 1$ TeV, we are able to suppress the Peskin-Takeuchi $S - T$ parameters [49,50] if we choose the lepton delocalization parameter x_ℓ to the value determined by the "ideal delocalization" [51]. As we will see later, the delocalization parameters x_q and x_ℓ are related with the W' couplings with quarks and leptons ξ_q and ξ_ℓ. Assuming the quark lepton universality of the W' coupling $\xi_q = \xi_\ell$, we are thus able to express the electroweak precision observable parameters in terms of $\xi_f = |\xi_q| = |\xi_\ell|$. In this section, we will also check whether or not the region in the $\xi_f - \xi_V$ plane favored by the ATLAS diboson anomalies is consistent with the electroweak precision measurements.

We have two neutral Higgs bosons in this model. One degree of freedom (h_1) of neural Higgs arises from Φ_1, the other (h_2) from Φ_2. The charged and pseudoscalar components of Φ_1 and Φ_2, i.e., π^a_1 and π^a_2 in (5.1) and (5.2) are all eaten by massive gauge bosons W, W', Z, and Z'. The 125 GeV Higgs boson h is considered to be a mixture of h_1 and h_2,

$$h = h_1 \cos\alpha + h_2 \sin\alpha, \tag{5.11}$$

where

$$S_1 = f_1 + h_1, \qquad S_2 = f_2 + h_2. \tag{5.12}$$

We are now ready to discuss the ATLAS 2 TeV diboson anomaly in the three-site moose model. There are three possible ways to obtain the hierarchy $M_{Z'}, M_{W'} = 2\ \text{TeV} \gg M_Z, M_W$ in this setup. One option is to take $g_{W1} \gg g_{W0}, g_{Y2}$ with keeping the VEVs $f_1 = f_2$ at the weak scale. Collider phenomenologies in this option were studied[3] in detail in Refs. [58–60]. This limit is theoretically interesting, because it can be regarded as an effective theory of strongly interacting Higgs sector [61–63] motivated by models of hidden local symmetry [64–68].

However, in order to realize 2 TeV $M_{W'}$ with this option, we need nonperturbatively strong g_{W1}. Reference [6] studies an interpretation of the ATLAS diboson anomaly with $g_{W1} \gg g_{W0}, g_{Y2}$, introducing higher order operators to suppress the effective coupling of the heavy vector resonance. We do not pursue this direction in this paper.

Other options are to take $f_1 \gg f_2$ or $f_1 \ll f_2$, keeping perturbative coupling constants g_{W0}, g_{W1}, and g_{Y2}. In the subsections below, we will give our results of $M_{W'}$, $M_{Z'}$, $g_{WWZ'}$, $g_{WZW'}$, g_{WWh}, and $g_{WW'h}$ in these limits and check the unitarity sum rules explicitly in this model. We will also point out that the reciprocality between ξ_f and ξ_V, suggested by the favored parameter regions of the ATLAS diboson anomaly fit, $\xi_V \simeq 3 \sim 5$, $\xi_f \simeq 0.2 \sim 0.3$ can be naturally realized in this setup.

A. $f_1 \gg f_2$

We start with the case $f_1 \gg f_2$. In this case the $SU(2)_{W0} \times SU(2)_{W1}$ gauge symmetry is broken into the diagonal subgroup at the high energy scale f_1, while the weak scale is given by f_2. We thus obtain the masses of W' and Z' in proportional to f_1,

$$M^2_{W'} \simeq M^2_{Z'} \simeq \frac{g^2_{W0} + g^2_{W1}}{4} f_1^2. \tag{5.13}$$

The weak $SU(2)$ gauge group at the weak scale should be the diagonal subgroup of $SU(2)_{W0} \times SU(2)_{W1}$, while the weak scale $U(1)_Y$ is given by $U(1)_{Y2}$. The gauge coupling strengths at the weak scale are therefore

$$g^2_W \simeq \frac{g^2_{W0} g^2_{W1}}{g^2_{W0} + g^2_{W1}}, \qquad g^2_Y \simeq g^2_{Y2}. \tag{5.14}$$

The masses of the W and Z bosons are given by

$$M^2_W \simeq \frac{g^2_W}{4} f_2^2, \qquad M^2_Z \simeq \frac{g^2_W + g^2_Y}{4} f_2^2. \tag{5.15}$$

It is easy to check these formulas by an explicit diagonalization of the mass matrices of the gauge fields W_0, W_1, and B, which are given by the Higgs kinetic term Lagrangian (5.8). We also obtain

[3]Hadron collider phenomenologies of narrow spin-1 resonances in the technicolor models are studied in Refs. [52,53]. The $f_1 = f_2$ model is believed to be a low energy effective description of the technicolor models. See also Refs. [54–57] for collider phenomenologies of technivector mesons in the low scale technicolor model.

$$M_{Z'}^2 - M_{W'}^2 = (M_Z^2 - M_W^2)\mathcal{O}\left(\frac{M_W^2}{M_{W'}^2}\right). \tag{5.16}$$

The W' and Z' bosons are therefore highly degenerated in this setup. We next consider the WZW' and WWZ' couplings. Explicit calculation of the mass diagonalization matrices of neutral and charged gauge bosons leads to

$$g_{WZW'} = \frac{g_{W1}}{g_{W0}} g_W \frac{M_W M_Z}{M_{W'}^2}, \tag{5.17}$$

and

$$g_{WWZ'} = \frac{g_{W1}}{g_{W0}} g_W \frac{M_W^2}{M_{Z'}^2}. \tag{5.18}$$

These results are perfectly consistent with our parametrization formulas (3.3) and (3.4). Therefore these couplings satisfy the unitarity and the custodial symmetry. Comparing (5.17), (5.18) with (3.3) and (3.4), we find ξ_V in this model is given by

$$\xi_V = \frac{g_{W1}}{g_{W0}}. \tag{5.19}$$

We also obtain $R = 1$, consistent with the custodial symmetry $M_{W'} = M_{Z'}$.

It is straightforward to calculate the Higgs couplings. We obtain

$$g_{WWh} \simeq g_W M_W \sin\alpha, \tag{5.20}$$

$$g_{WW'h} \simeq -\frac{g_{W1}}{g_{W0}} g_W M_W \sin\alpha, \tag{5.21}$$

$$g_{ZZ'h} \simeq -\frac{g_{W1}}{g_{W0}} g_W M_Z \sin\alpha. \tag{5.22}$$

Again, these results are consistent with our custodial symmetry formulas (3.5) and (3.6) and the result of the unitarity sum rules (3.7). The parameter ξ_h and κ_V in this model are given by

$$\xi_h = -\frac{g_{W1}}{g_{W0}} \sin\alpha, \tag{5.23}$$

$$\kappa_V = \sin\alpha. \tag{5.24}$$

We next calculate the W' and Z' couplings with the quarks and the leptons. We find that both the quark hypercharge current and the lepton hypercharge current couple with the Z' boson only with coefficients suppressed by $(M_Z^2 - M_W^2)/M_{W'}^2$. The couplings of W' and Z' with the quarks and the leptons are therefore consistent with the ansatz given in Sec. III. The parameters ξ_q and ξ_ℓ are given by

$$\xi_q = \frac{g_{W0}}{g_{W1}}\left(1 - x_q - x_q \frac{g_{W1}^2}{g_{W0}^2}\right), \tag{5.25}$$

$$\xi_\ell = \frac{g_{W0}}{g_{W1}}\left(1 - x_\ell - x_\ell \frac{g_{W1}^2}{g_{W0}^2}\right), \tag{5.26}$$

with x_q, x_ℓ being the delocalization parameters for the quarks and the leptons. We note that, if the delocalization parameters are small enough $x_q \lesssim g_{W0}^2/g_{W1}^2$, ξ_V and $\xi_q(\xi_\ell)$ satisfy the relation

$$\xi_V \xi_q \lesssim 1. \tag{5.27}$$

Note that this relation is consistent with our result presented in Sec. IV. The three-site model with $g_{W0}/g_{W1} \simeq 0.25$ gives the reference value cross section for the ATLAS diboson anomalies without causing conflicts with other limits on W' and Z'. The κ_V is smaller than unity in this model, however. We need to take care of the consistency with the signal strengths in the Higgs production measurements as done in Ref. [19].

The electroweak precision observable parameters are evaluated at the tree level as

$$\hat{S} \simeq \frac{M_W^2}{M_{W'}^2}\xi_V \xi_f, \qquad W \simeq \frac{M_W^2}{M_{W'}^2}\xi_f^2. \tag{5.28}$$

Here we used the notation of Ref. [69]. We assumed $\xi_f = |\xi_q| = |\xi_\ell|$ and neglected terms suppressed by $1/\xi_V$ or ξ_f in (5.28), given the situation that $\xi_V \simeq 3 \sim 4$ and $\xi_f \simeq 0.2 \sim 0.3$ are favored in the fit for the ATLAS diboson anomalies. The analysis of Ref. [69] shows that $\hat{S}$ and W need to be smaller than a few permil in order to satisfy the electroweak precision constraints. Note that both $\hat{S}$ and W are suppressed by $M_W^2/M_{W'}^2 \simeq 1.6 \times 10^{-3}$ in (5.28) and vanish in the ideal delocalization limit $\xi_f = 0$. Thanks to the suppression factor $M_W^2/M_{W'}^2$, the explanation of the ATLAS diboson anomaly is marginally consistent with the electroweak precision measurements at the tree level.

There also exist orders of a few permil loop corrections to the electroweak precision parameters. However, these loop corrections depend on the assumptions of the UV completion behind the fermion delocalization. For an example, the fermion delocalization can be UV-completed by introducing additional heavy fermions. The loop level corrections to the electroweak precision parameters depend on the mass spectrum of the heavy additional fermions. See, e.g., Ref. [70]. Since we do not specify such a UV-completion in this paper, we do not consider loop level constraints any further.

B. $f_1 \ll f_2$

The case $f_1 \ll f_2$ can be studied in a similar manner. In this case the $SU(2)_{W1} \times U(1)_{Y2}$ group is broken to $U(1)_Y$ at the high energy scale f_2, while the $SU(2)_{W0} \times U(1)_Y$ is broken by f_1 at the weak scale. The masses of W' and Z' are therefore given by

$$M_{W'}^2 \simeq \frac{1}{4} g_{W1}^2 f_2^2, \tag{5.29}$$

$$M_{Z'}^2 \simeq \frac{1}{4}(g_{W1}^2 + g_{Y2}^2) f_2^2. \tag{5.30}$$

The Z' boson is heavier and can be separated from W' at the LHC experiments. The model in this limit therefore corresponds to the nondegenerated case in Sec. IV of this paper. Since the weak hypercharge gauge boson at the weak scale is a mixture of the $SU(2)_{W1}$ and $U(1)_{Y2}$ gauge bosons, the gauge coupling strengths at the weak scale are given by

$$g_W^2 \simeq g_{W0}^2, \qquad g_Y^2 \simeq \frac{g_{W1}^2 g_{Y2}^2}{g_{W1}^2 + g_{Y2}^2}, \tag{5.31}$$

and we obtain the weak gauge boson mass,

$$M_W^2 \simeq \frac{g_W^2}{4} f_1^2, \qquad M_Z^2 \simeq \frac{g_W^2 + g_Y^2}{4} f_1^2. \tag{5.32}$$

The WZW', WWZ', WWh, $WW'h$, $ZZ'h$ couplings are given by

$$g_{WZW'} = \frac{g_{W1}}{g_{W0}} g_W \frac{M_W M_Z}{M_{W'}^2}, \tag{5.33}$$

$$g_{WWZ'} = \frac{g_{W1}}{g_{W0}} g_W \frac{M_W^2}{M_{Z'}^2} \frac{M_{W'}}{M_{Z'}}, \tag{5.34}$$

$$g_{WWh} \simeq g_W M_W \cos\alpha, \tag{5.35}$$

$$g_{WW'h} \simeq \frac{g_{W1}}{g_{W0}} g_W M_W \cos\alpha, \tag{5.36}$$

$$g_{ZZ'h} \simeq \frac{g_{W1}}{g_{W0}} g_W M_Z \frac{M_{W'}}{M_{Z'}} \cos\alpha, \tag{5.37}$$

which are consistent with our unitarity and custodial symmetry formulas (3.3), (3.4), (3.5), (3.6), and (3.7). The parameters ξ_V, ξ_h,κ_V, and R are given by

$$\xi_V = \frac{g_{W1}}{g_{W0}} \tag{5.38}$$

$$\xi_h = \frac{g_{W1}}{g_{W0}} \cos\alpha \tag{5.39}$$

$$\kappa_V = \cos\alpha, \tag{5.40}$$

and

$$R = \frac{M_{W'}}{M_{Z'}}. \tag{5.41}$$

The Z' boson does couple with the fermion hypercharge currents in this setup. Therefore the couplings of Z' with quarks and leptons cannot be parametrized by the parameters ξ_q and ξ_ℓ. The Z' boson becomes heavier enough than $M_{W'} = 2$ TeV, however, and therefore irrelevant in the explanation of the ATLAS diboson anomalies. In the phenomenological analysis, we therefore use the parameters which describe the W' coupling with quarks and leptons,

$$\xi_q = -\frac{g_{W1}}{g_{W0}} x_q, \tag{5.42}$$

$$\xi_\ell = -\frac{g_{W1}}{g_{W0}} x_\ell. \tag{5.43}$$

We find that the relatively small value of $|\xi_q| \simeq 0.3$, which is favored by the W' constraints, is possible if we take $x_q \lesssim g_{W0}^2/g_{W1}^2$.

We find a nondecoupling tree level correction

$$\hat{S} \simeq -\frac{\xi_f}{\xi_V}, \tag{5.44}$$

which is not suppressed by $M_W^2/M_{W'}^2$ in the $f_1 \ll f_2$ model in contrast to the $f_1 \gg f_2$ case. The constraint from the electroweak precision parameters is therefore much more severe than the $f_1 \gg f_2$ case in this setup. Again we assumed $\xi_f = |\xi_q| = |\xi_\ell|$ and neglected terms suppressed by $1/\xi_V$ or ξ_f. For $\xi_V \simeq 3 \sim 5$ and $\xi_f \simeq 0.2 \sim 0.3$, we find $\hat{S} \simeq 0.1$, clearly contradicting with the present experimental limit on $\hat{S}$, namely $|\hat{S}| \lesssim 10^{-3}$ [69]. The three-site moose model with $f_1 \ll f_2$ is therefore ruled out as an interpretation of the ATLAS diboson anomaly at least for the quark-lepton universal coupling case $\xi_q = \xi_\ell$.

VI. SUMMARY

In this paper, we have studied general structures of perturbative W' models from the viewpoint of unitarity sum rules and the custodial $SU(2)$ symmetry. We found that the unitarity sum rules and the custodial symmetry are powerful enough, to predict many relations among WWZ', WZW', WWh, $WW'h$, and $ZZ'h$ coupling strengths. Especially, we derived a novel relation (2.29) from these sum rules, which can be applied to a large class of perturbative models including arbitrary numbers of the heavy vector triplet bosons and neutral Higgs bosons. Using these relations, we surveyed parameter space of W' models to search for the region possible to explain the ATLAS 2 TeV diboson anomalies. If the CMS excesses at 1.8 TeV are not related with the ATLAS 2 TeV anomalies,

and if the 125 GeV Higgs boson is the SM-like Higgs boson, we found that the CMS upper limit on the $W' \to Wh$ channel at 2 TeV is hardly compatible with the ATLAS 2 TeV diboson anomalies, suggesting non-SM-like properties of the 125 GeV Higgs boson. Based on the three-site moose model Lagrangian, we then provided a couple of example models of non-SM-like Higgs bosons, which may be able to explain the ATLAS diboson anomalies.

We emphasize that the three-site moose model we used in this paper should be regarded merely as an example to illustrate the properties of models which may explain the ATLAS 2 TeV diboson anomalies. Models having similar properties (the non-SM-like Higgs and the delocalization of the fermion weak current) such as the extra dimension models, the partial compositeness models [47], the top triangle moose models [71,72], and the composite Higgs models [73–76] should be studied further. Note that the proof of the relation (2.29) we provided in this paper is directly applicable only in a category of perturbative models with the custodial symmetry containing arbitrary numbers of heavy vector triplet and neutral Higgs bosons. Although this category of models already covers wide varieties of interesting models, there also exist phenomenologically viable models which do not belong to this category. It is particularly interesting to study the W' phenomenology in these nonperturbative models.

Each of ATLAS and CMS experiments will accumulate $\sim 10\ \mathrm{fb}^{-1}$ luminosity within year 2015 run at $\sqrt{s} = 13$ TeV. If the ATLAS diboson anomalies are settled to exist in these LHC Run2 experiments, the next target is to clarify the properties of the 2 TeV diboson resonance. Especially, as we stressed in this paper, its Vh decay channel ($V = W$ or Z) becomes important, since it can determine whether the 125 GeV Higgs particle is SM-like or not.

ACKNOWLEDGMENTS

We thank Junji Hisano, Sekhar R. Chivukula, Hidenori Fukano, Masafumi Kurachi, Shinya Matsuzaki, and Koichi Yamawaki for useful discussions and valuable comments. T. A.'s work is supported by Grant-in-Aid for Scientific research from the Ministry of Education, Culture, Sports, Science and Technology (MEXT), Japan, No. 23104006. R. N.'s work is supported by Research Fellowships of the Japan Society for the Promotion of Science (JSPS) for Young Scientists No. 263947. M. T.'s work is supported in part by the JSPS Grant-in-Aid for Scientific Research No. 15K05047.

Note added.—After we sent our first version of manuscript to the arXiv, a study on the unitarity implications for the ATLAS diboson anomalies had appeared [17], in which the $WW \to WW$ sum rule (2.18) was used to constrain the WWh coupling.

[1] G. Aad *et al.* (ATLAS Collaboration), Search for high-mass diboson resonances with boson-tagged jets in proton-proton collisions at $\sqrt{s} = 8$ TeV with the ATLAS detector, arXiv:1506.00962.
[2] V. Khachatryan *et al.* (CMS Collaboration), Search for massive resonances in dijet systems containing jets tagged as W or Z boson decays in pp collisions at $\sqrt{s} = 8$ TeV, J. High Energy Phys. 08 (2014) 173.
[3] G. Aad *et al.* (ATLAS Collaboration), Search for production of WW/WZ resonances decaying to a lepton, neutrino and jets in pp collisions at $\sqrt{s} = 8$ TeV with the ATLAS detector, Eur. Phys. J. C **75**, 209 (2015); **75**, 370 (2015).
[4] V. Khachatryan *et al.* (CMS Collaboration), Search for a massive resonance decaying into a Higgs boson and a W or Z boson in hadronic nal states in proton-proton collisions at $\sqrt{s} = 8$ TeV, arXiv:1506.01443.
[5] CMS Collaboration, Report No. CMS PAS EXO-14-010.
[6] H. S. Fukano, M. Kurachi, S. Matsuzaki, K. Terashi, and K. Yamawaki, 2 TeV walking technirho at LHC?, arXiv:1506.03751.
[7] J. Hisano, N. Nagata, and Y. Omura, Interpretations of the ATLAS diboson resonances, arXiv:1506.03931.
[8] D. B. Franzosi, M. T. Frandsen, and F. Sannino, Diboson signals via fermi scale spin-one states, arXiv:1506.04392.
[9] K. Cheung, W. Y. Keung, P. Y. Tseng, and T. C. Yuan, Interpretations of the ATLAS diboson anomaly, arXiv:1506.06064.
[10] B. A. Dobrescu and Z. Liu, A W' boson near 2 TeV: Predictions for Run 2 of the LHC, arXiv:1506.06736.
[11] J. A. Aguilar-Saavedra, Triboson interpretations of the ATLAS diboson excess, arXiv:1506.06739.
[12] A. Alves, A. Berlin, S. Profumo, and F. S. Queiroz, Dirac-Fermionic dark matter in $U(1)_X$ models, arXiv:1506.06767.
[13] Y. Gao, T. Ghosh, K. Sinha, and J. H. Yu, G221 interpretations of the diboson and Wh excesses, arXiv:1506.07511.
[14] A. Thamm, R. Torre, and A. Wulzer, A composite Heavy Vector Triplet in the ATLAS di-boson excess, arXiv:1506.08688.
[15] J. Brehmer, J. Hewett, J. Kopp, T. Rizzo, and J. Tattersall, Symmetry restored in dibosons at the LHC?, arXiv:1507.00013.
[16] Q. H. Cao, B. Yan, and D. M. Zhang, Simple non-abelian extensions and diboson excesses at the LHC, arXiv:1507.00268.

[17] G. Cacciapaglia and M. T. Frandsen, Unitarity implications of diboson resonance in the TeV region for Higgs physics, arXiv:1507.00900.
[18] D. Pappadopulo, A. Thamm, R. Torre, and A. Wulzer, Heavy vector triplets: bridging theory and data, J. High Energy Phys. 09 (2014) 060.
[19] T. Abe, N. Chen, and H. J. He, LHC Higgs signatures from extended electroweak gauge symmetry, J. High Energy Phys. 01 (2013) 082.
[20] R. S. Chivukula, B. Coleppa, S. Di Chiara, E. H. Simmons, H. J. He, M. Kurachi, and M. Tanabashi, A Three site Higgsless model, Phys. Rev. D **74**, 075011 (2006).
[21] N. Arkani-Hamed, A. G. Cohen, and H. Georgi, (De) constructing Dimensions, Phys. Rev. Lett. **86**, 4757 (2001).
[22] C. T. Hill, S. Pokorski, and J. Wang, Gauge invariant effective Lagrangian for Kaluza-Klein modes, Phys. Rev. D **64**, 105005 (2001).
[23] C. Csaki, C. Grojean, H. Murayama, L. Pilo, and J. Terning, Gauge theories on an interval: Unitarity without a Higgs boson, Phys. Rev. D **69**, 055006 (2004).
[24] J. M. Cornwall, D. N. Levin, and G. Tiktopoulos, Uniqueness of Spontaneously Broken Gauge Theories, Phys. Rev. Lett. **30**, 1268 (1973); **31**, 572(E) (1973).
[25] J. M. Cornwall, D. N. Levin, and G. Tiktopoulos, Derivation of gauge invariance from high-energy unitarity bounds on the S matrix, Phys. Rev. D **10**, 1145 (1974); **11**, 972(E) (1975).
[26] C. H. Llewellyn Smith, High energy behaviour and gauge symmetry, Phys. Lett. **46B**, 233 (1973).
[27] J. F. Gunion, H. E. Haber, and J. Wudka, Sum rules for Higgs bosons, Phys. Rev. D **43**, 904 (1991).
[28] R. S. Chivukula, H. J. He, M. Kurachi, E. H. Simmons, and M. Tanabashi, General sum rules for WW scattering in Higgsless models: Equivalence theorem and deconstruction identities, Phys. Rev. D **78**, 095003 (2008).
[29] R. Foadi, M. Jarvinen, and F. Sannino, Unitarity in technicolor, Phys. Rev. D **79**, 035010 (2009).
[30] A. E. Carcamo Hernandez and R. Torre, A 'composite' scalar-vector system at the LHC, Nucl. Phys. **B841**, 188 (2010).
[31] B. Bellazzini, C. Csaki, J. Hubisz, J. Serra, and J. Terning, Composite Higgs sketch, J. High Energy Phys. 11 (2012) 003.
[32] C. Englert, P. Harris, M. Spannowsky, and M. Takeuchi, Unitarity-controlled resonances after the Higgs boson discovery, Phys. Rev. D **92**, 013003 (2015).
[33] B. W. Lee, C. Quigg, and H. B. Thacker, Weak interactions at very high energies: The role of the Higgs-boson mass, Phys. Rev. D **16**, 1519 (1977).
[34] T. Sjostrand, S. Mrenna, and P. Z. Skands, A brief introduction to PYTHIA 8.1, Comput. Phys. Commun. **178**, 852 (2008).
[35] G. Altarelli, B. Mele, and M. Ruiz-Altaba, Searching for new heavy vector bosons in $p\bar{p}$ colliders, Z. Phys. C **45**, 109 (1989); Z. Phys. C **47**, 676 (1990).
[36] G. Aad *et al.* (ATLAS Collaboration), Search for new particles in events with one lepton and missing transverse momentum in pp collisions at $\sqrt{s} = 8$ TeV with the ATLAS detector, J. High Energy Phys. 09 (2014) 037.
[37] V. Khachatryan *et al.* (CMS Collaboration), Search for physics beyond the standard model in final states with a lepton and missing transverse energy in proton-proton collisions at $\sqrt{s} = 8$ TeV, Phys. Rev. D **91**, 092005 (2015).
[38] G. Aad *et al.* (ATLAS Collaboration), Search for high-mass dilepton resonances in pp collisions at $\sqrt{s} = 8$ TeV with the ATLAS detector, Phys. Rev. D **90**, 052005 (2014).
[39] V. Khachatryan *et al.* (CMS Collaboration), Search for physics beyond the standard model in dilepton mass spectra in proton-proton collisions at $\sqrt{s} = 8$ TeV, J. High Energy Phys. 04 (2015) 025.
[40] G. Aad *et al.* (ATLAS Collaboration), Search for new phenomena in the dijet mass distribution using pp collision data at $\sqrt{s} = 8$ TeV with the ATLAS detector, Phys. Rev. D **91**, 052007 (2015).
[41] V. Khachatryan *et al.* (CMS Collaboration), Search for resonances and quantum black holes using dijet mass spectra in proton-proton collisions at $\sqrt{s} = 8$ TeV, Phys. Rev. D **91**, 052009 (2015).
[42] J. Pumplin, D. R. Stump, J. Huston, H. L. Lai, P. M. Nadolsky, and W. K. Tung, New generation of parton distributions with uncertainties from global QCD analysis, J. High Energy Phys. 07 (2002) 012.
[43] R. S. Chivukula, D. A. Dicus, and H. J. He, Unitarity of compactified five-dimensional Yang-Mills theory, Phys. Lett. B **525**, 175 (2002).
[44] R. S. Chivukula and H. J. He, Unitarity of deconstructed five-dimensional Yang-Mills theory, Phys. Lett. B **532**, 121 (2002).
[45] H. Georgi, A tool kit for builders of composite models, Nucl. Phys. **B266**, 274 (1986).
[46] G. Cacciapaglia, C. Csaki, C. Grojean, and J. Terning, Curing the ills of Higgsless models: The S parameter and unitarity, Phys. Rev. D **71**, 035015 (2005).
[47] D. B. Kaplan, Flavor at SSC energies: A New mechanism for dynamically generated fermion masses, Nucl. Phys. **B365**, 259 (1991).
[48] T. Abe, R. S. Chivukula, E. H. Simmons, and M. Tanabashi, Flavor structure of the three-site Higgsless model, Phys. Rev. D **85**, 035015 (2012).
[49] M. E. Peskin and T. Takeuchi, New Constraint on a Strongly Interacting Higgs Sector, Phys. Rev. Lett. **65**, 964 (1990).
[50] M. E. Peskin and T. Takeuchi, Estimation of oblique electroweak corrections, Phys. Rev. D **46**, 381 (1992).
[51] R. S. Chivukula, E. H. Simmons, H. J. He, M. Kurachi, and M. Tanabashi, Ideal fermion delocalization in Higgsless models, Phys. Rev. D **72**, 015008 (2005).
[52] E. Eichten, I. Hinchliffe, K. D. Lane, and C. Quigg, Super collider physics, Rev. Mod. Phys. **56**, 579 (1984); **58**, 1065 (1986).
[53] K. D. Lane and M. V. Ramana, Walking technicolor signatures at hadron colliders, Phys. Rev. D **44**, 2678 (1991).
[54] E. Eichten and K. D. Lane, Low-scale technicolor at the Tevatron, Phys. Lett. B **388**, 803 (1996).
[55] K. D. Lane, Technihadron production and decay in low-scale technicolor, Phys. Rev. D **60**, 075007 (1999).

[56] K. Lane and S. Mrenna, Collider phenomenology of technihadrons in the technicolor straw man model, Phys. Rev. D **67**, 115011 (2003).
[57] E. Eichten and K. Lane, Low-scale technicolor at the Tevatron and LHC, Phys. Lett. B **669**, 235 (2008).
[58] H. J. He, Y. P. Kuang, Y. H. Qi, B. Zhang, A. Belyaev, R. S. Chivukula, N. D. Christensen, A. Pukhov, and E. H. Simmons, CERN LHC signatures of new gauge bosons in minimal Higgsless model, Phys. Rev. D **78**, 031701 (2008).
[59] T. Abe, T. Masubuchi, S. Asai, and J. Tanaka, Drell-Yan production of Z' in the three-site Higgsless model at the LHC, Phys. Rev. D **84**, 055005 (2011).
[60] C. Du, H. J. He, Y. P. Kuang, B. Zhang, N. D. Christensen, R. S. Chivukula, and E. H. Simmons, Discovering new gauge bosons of electroweak symmetry breaking at LHC-8, Phys. Rev. D **86**, 095011 (2012).
[61] R. Casalbuoni, S. De Curtis, D. Dominici, and R. Gatto, Effective weak interaction theory with a possible new vector resonance from a strong higgs sector, Phys. Lett. **155B**, 95 (1985).
[62] R. Casalbuoni, D. Dominici, A. Deandrea, R. Gatto, S. De Curtis, and M. Grazzini, Low energy strong electroweak sector with decoupling, Phys. Rev. D **53**, 5201 (1996).
[63] K. Lane and A. Martin, Effective Lagrangian for low-scale technicolor, Phys. Rev. D **80**, 115001 (2009).
[64] M. Bando, T. Kugo, S. Uehara, K. Yamawaki, and T. Yanagida, Is the ρ Meson a Dynamical Gauge Boson of Hidden Local Symmetry, Phys. Rev. Lett. **54**, 1215 (1985).
[65] M. Bando, T. Kugo, and K. Yamawaki, On the vector mesons as dynamical gauge bosons of hidden local symmetries, Nucl. Phys. **B259**, 493 (1985).
[66] M. Bando, T. Fujiwara, and K. Yamawaki, Generalized hidden local symmetry and the A_1 meson, Prog. Theor. Phys. **79**, 1140 (1988).
[67] M. Bando, T. Kugo, and K. Yamawaki, Nonlinear realization and hidden local symmetries, Phys. Rep. **164**, 217 (1988).
[68] M. Harada and K. Yamawaki, Hidden local symmetry at loop: A new perspective of composite gauge boson and chiral phase transition, Phys. Rep. **381**, 1 (2003).
[69] R. Barbieri, A. Pomarol, R. Rattazzi, and A. Strumia, Electroweak symmetry breaking after LEP-1 and LEP-2, Nucl. Phys. **B703**, 127 (2004).
[70] T. Abe, S. Matsuzaki, and M. Tanabashi, Does the three site Higgsless model survive the electroweak precision tests at loop?, Phys. Rev. D **78**, 055020 (2008).
[71] R. Sekhar Chivukula, N. D. Christensen, B. Coleppa, and E. H. Simmons, The top triangle moose: Combining Higgsless and topcolor mechanisms for mass generation, Phys. Rev. D **80**, 035011 (2009).
[72] T. Abe and R. Kitano, Phenomenology of partially composite standard model, Phys. Rev. D **88**, 015019 (2013).
[73] D. K. Hong, S. D. H. Hsu, and F. Sannino, Composite Higgs from higher representations, Phys. Lett. B **597**, 89 (2004).
[74] K. Agashe, R. Contino, and A. Pomarol, The minimal composite Higgs model, Nucl. Phys. **B719**, 165 (2005).
[75] S. Matsuzaki and K. Yamawaki, Techni-dilaton at 125 GeV, Phys. Rev. D **85**, 095020 (2012).
[76] K. Lane, A composite Higgs model with minimal fine-tuning: The large-N and weak-technicolor limit, Phys. Rev. D **90**, 095025 (2014).